Sphingosine kinases and their metabolites modulate endolysosomal trafficking in photoreceptors

Ikuko Yonamine,[1,2] Takeshi Bamba,[3] Niraj K. Nirala,[1,2] Nahid Jesmin,[1,2] Teresa Kosakowska-Cholody,[4] Kunio Nagashima,[5] Eiichiro Fukusaki,[3] Jairaj K. Acharya,[4] and Usha Acharya[1,2]

[1]Program in Gene Function and Expression and [2]Program in Molecular Medicine, University of Massachusetts Medical School, Worcester, MA 01605
[3]Department of Biotechnology, Graduate School of Engineering, Osaka University, Osaka 565-0871, Japan
[4]Laboratory of Cell and Developmental Signaling, National Cancer Institute, Frederick, MD 21702
[5]Electron Microscopy Facility and Image Analysis Laboratory, Science Applications International Corporation–Frederick, Frederick, MD 21702

Internalized membrane proteins are either transported to late endosomes and lysosomes for degradation or recycled to the plasma membrane. Although proteins involved in trafficking and sorting have been well studied, far less is known about the lipid molecules that regulate the intracellular trafficking of membrane proteins. We studied the function of sphingosine kinases and their metabolites in endosomal trafficking using *Drosophila melanogaster* photoreceptors as a model system. Gain- and loss-of-function analyses show that sphingosine kinases affect trafficking of the G protein–coupled receptor Rhodopsin and the light-sensitive transient receptor potential (TRP) channel by modulating the levels of dihydrosphingosine 1 phosphate (DHS1P) and sphingosine 1 phosphate (S1P). An increase in DHS1P levels relative to S1P leads to the enhanced lysosomal degradation of Rhodopsin and TRP and retinal degeneration in wild-type photoreceptors. Our results suggest that sphingosine kinases and their metabolites modulate photoreceptor homeostasis by influencing endolysosomal trafficking of Rhodopsin and TRP.

Introduction

Sphingolipids are integral components of membranes, and several of them, such as ceramide, sphingosine, and sphingosine 1 phosphate (S1P), serve as second messengers regulating diverse processes, including growth, differentiation, apoptosis, and angiogenesis (Dickson et al., 2006; Hannun and Obeid, 2008; Maceyka et al., 2009). Enzymes involved in the generation and conversion of these sphingolipids are conserved across species, including *Drosophila melanogaster* (Acharya and Acharya, 2005; Futerman and Riezman, 2005). Sphingosine kinases are penultimate enzymes in the sphingolipid biosynthetic pathway that phosphorylate sphingosine to S1P, and two distinct isoforms have been identified in mammals, flies, worms, yeast, and plants (Kohama et al., 1998; Liu et al., 2000; Pitson et al., 2000a). Sphingosine kinases also phosphorylate dihydrosphingosine (DHS) and produce DHS 1 phosphate (DHS1P). A large volume of literature has established the participation of these kinases in many signaling pathways (Olivera and Spiegel, 1993; Hait et al., 2006; Alemany et al., 2007; Pyne et al., 2009). S1P not only acts as an intracellular messenger but also as an extracellular ligand for a family of G protein–coupled S1P receptors (S1P-GPCRs; Sanchez and Hla, 2004). By binding to these receptors, S1P regulates angiogenesis, cardiac development, and lymphocyte egress from the thymus. However, a clear distinction of the intracellular and extracellular roles of these kinases and S1P has not yet emerged. *Drosophila* lack S1P-GPCRs and, therefore, could serve as a good system to dissect intracellular functions of sphingosine kinases and their metabolites.

Drosophila phototransduction is a prototypic GPCR-signaling cascade that begins with the absorption of light by Rhodopsin followed by activation of $G\alpha_q$. $G\alpha_q$ activates NORPA, eventually leading to the gating of transient receptor potential (TRP) and TRP-like channels (Hardie and Raghu, 2001; Wang and Montell, 2007). Like many GPCRs, Rhodopsin 1 (Rh1)

Correspondence to Usha Acharya: usha.acharya@umassmed.edu

Abbreviations used in this paper: DHS, dihydrosphingosine; DHS1P, DHS 1 phosphate; GMR, glass multimer reporter; GPCR, G protein–coupled receptor; IPP, inositol polyphosphate 1 phosphatase; Rh1, Rhodopsin 1; S1P, sphingosine 1 phosphate; TRP, transient receptor potential; UAS, upstream activating sequence; UFLC MS/MS, ultrafast liquid chromatography coupled to tandem mass spectrometry.

The Rockefeller University Press $30.00
J. Cell Biol. Vol. 192 No. 4 557–567
www.jcb.org/cgi/doi/10.1083/jcb.201004098

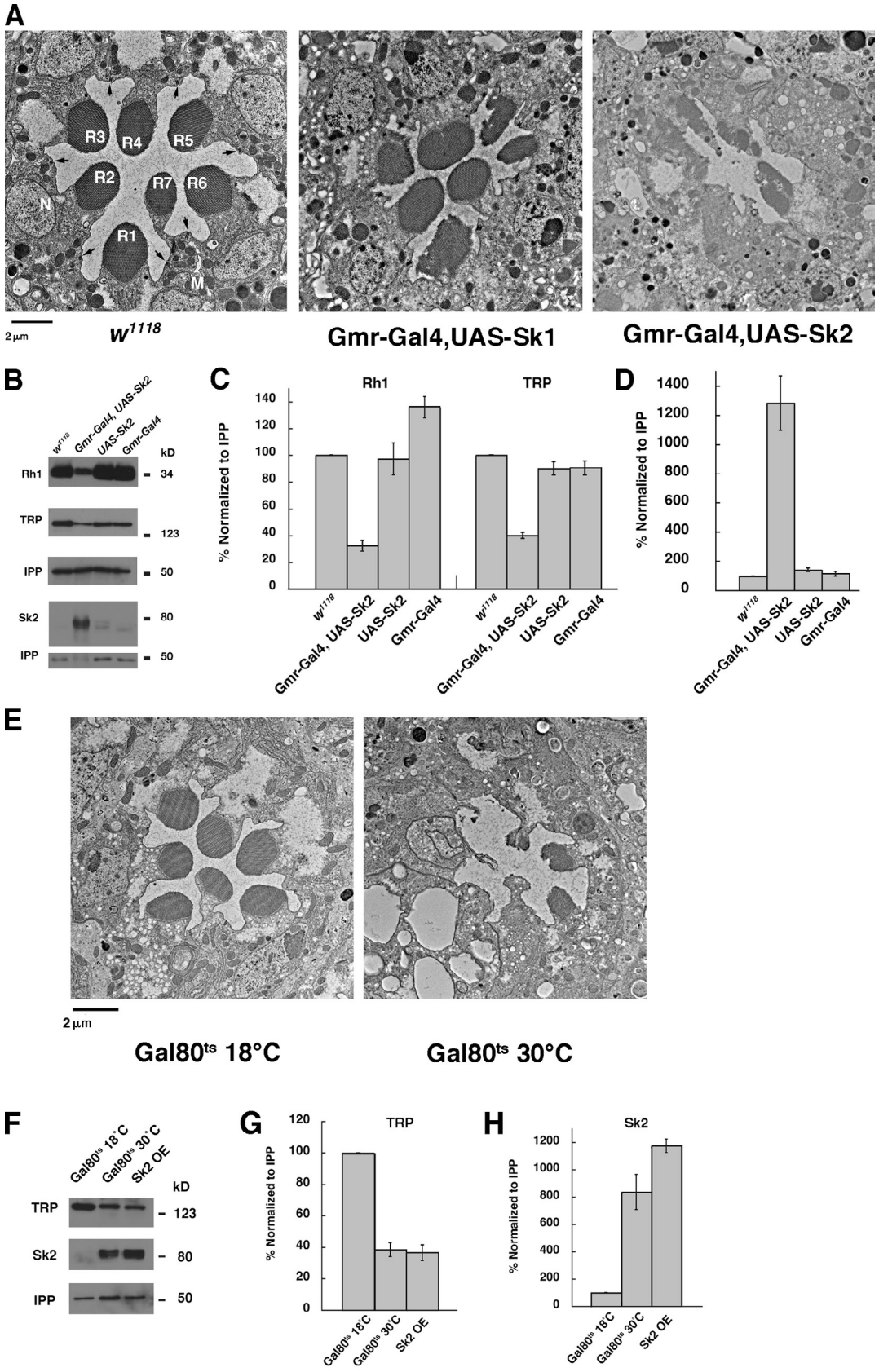

Figure 1. **Targeted expression of Sk2 leads to photoreceptor degeneration and decrease in Rh1 and TRP levels.** (A) 7-d-old photoreceptors overexpressing Sk1 show a mild effect on rhabdomeres, whereas photoreceptors overexpressing Sk2 show severe degeneration. The percentage of intact rhabdomeres for w^{1118} is 100%, for Sk1 overexpression is 80%, and for Sk2 overexpression is 4%. R1–R7 label the rhabdomeres of R1–R7 photoreceptor cells;

undergoes internalization and degradation after activation in *Drosophila* photoreceptors (Acharya et al., 2004; Xu et al., 2004; Orem et al., 2006; Chinchore et al., 2009). Perturbation of the endocytic regulation of Rh1 leads to retinal degeneration of photoreceptors (Alloway et al., 2000, Kiselev et al., 2000). In the endocytic pathway, some membrane proteins recycle from endosomes to the plasma membrane, whereas others are transported to lysosomes for degradation. The endolysosomal system is viewed as a mosaic of different membrane domains with different protein and lipid compositions (Mukherjee and Maxfield, 2000; Gruenberg, 2003). Although we know a lot about protein families that dictate trafficking and sorting, comparatively, less is known about lipid determinants involved in trafficking processes. Phospholipids, such as phosphatidylinositol 3 phosphate and its effector proteins, mediate endosomal receptor sorting and intraluminal vesicle formation (Odorizzi et al., 2000; Birkeland and Stenmark, 2004). Studies on Sec 14 and Sec 14–like phosphatidylinositol transfer proteins have revealed how this family of lipid-modifying proteins integrates lipid metabolism with signaling and membrane trafficking (Mousley et al., 2007; Bankaitis et al., 2010). Bis(monoacylglycero)phosphate is rich in late endosomes and lysosomes and involved in the biogenesis, organization, and dynamics of these organelles (Kobayashi et al., 2002; Schulze et al., 2009). Diacylglycerol regulates protein transport from the Golgi to the cell surface in yeast and mammalian cells (Kearns et al., 1997; Baron and Malhotra, 2002). Sterols are involved in endolysosomal trafficking by promoting the formation of specialized membrane domains (Pichler and Riezman, 2004). Among sphingolipids, glucosylceramide is involved in the sorting of melanosomal enzymes from lysosomal membrane proteins, and ceramide is required for the formation of exosomes (Groux-Degroote et al., 2008; Trajkovic et al., 2008).

In this study, gain- and loss-of-function analyses of Sk1 (*Drosophila* sphingosine kinase 1) and Sk2 sphingosine kinases in photoreceptors show that they modulate the endolysosomal trafficking of Rh1 and TRP. A relative increase in DHS1P over S1P enhances the lysosomal degradation of Rh1 and TRP and induces photoreceptor degeneration. Our results suggest that sphingosine kinases regulate photoreceptor homeostasis by maintaining a balance between DHS1P and S1P.

Results and discussion

Targeted expression of *Drosophila* Sk2, but not Sk1, leads to the severe degeneration of photoreceptors

Recently, we have reported on the functional significance of the sphingolipid-metabolizing enzymes ceramidase and ceramide kinase in *Drosophila* photoreceptors (Acharya et al., 2008, Dasgupta et al., 2009). In these and earlier experiments, we showed that ceramide level is important for photoreceptor viability and function (Acharya et al., 2003). Therefore, we decided to analyze enzymes and metabolites downstream of ceramide in this process. Sphingosine kinases catalyze the conversion of sphingosine to S1P, and two isoforms, Sk1 and Sk2, have been characterized in *Drosophila* (Herr et al., 2004). *Drosophila* Sk1 and Sk2 proteins are 39% identical and 63% similar to each other, and expression of either of these isoforms could functionally complement a yeast mutant deficient in Sk activity (Herr et al., 2004). Western blots of retinal extracts probed with antibodies to either Sk1 or Sk2 show that both are expressed in the eye (Fig. S1 A). We performed targeted overexpression of Sk1 and Sk2 in the *Drosophila* eye using a glass multimer reporter (GMR) Gal4 driver. Electron micrographs of photoreceptors show that expression of Sk1 does not disturb ommatidial architecture, whereas mild effects are seen on rhabdomere organization (Fig. 1 A). Expression of Sk2 leads to extensive photoreceptor degeneration: very few intact ommatidia are seen, rhabdomeres are lost, and cells are vacuolated. To ensure that the enzymatic activity of Sk2 is required for the observed degeneration, we generated transgenic flies expressing a catalytically inactive form of Sk2. Amino acid substitutions in a conserved diacylglycerol kinase catalytic domain of human sphingosine kinases (residues 270–288 of human Sphk2 [mammalian sphingosine kinase 2]) have been shown to result in catalytically inactive enzymes (Pitson et al., 2000b; Herr et al., 2004). We introduced substitutions ($GSGN^{312–315}$ to DDDD) in the corresponding conserved domain of *Drosophila* Sk2 and generated transgenic flies. Targeted overexpression of this mutant form of Sk2 does not lead to photoreceptor degeneration (Fig. S1, B and C).

Enhanced lysosomal degradation of Rh1 and TRP in Sk2 overexpressors

Because S1P is a known second messenger in GPCR signaling, we decided to test whether S1P targets any of the known phototransduction components. Analysis of the steady-state levels of various phototransduction components by Western analysis reveals that Rh1 and TRP levels are significantly reduced in these flies (Fig. 1, B–D). However, Rh1 and TRP levels are not reduced in transgenic flies overexpressing inactive Sk2 (Fig. S1 C). The levels of other phototransduction components, such as Gα, INAD, arrestin 2 (Arr2), and NinaC, are not affected as compared with Rh1 and TRP in functional Sk2 overexpressors (Fig. S2 A). Two lines of experiments suggest that Rh1 and TRP are not arrested in the secretory pathway but traffic to the plasma membrane in flies overexpressing functional Sk2. Immunolocalization of Rh1 and TRP in retinae of newly eclosed Sk2

N represents the nucleus, M represents mitochondria, and black arrows show adherens junctions. (B) Sk2 overexpression results in decreased Rh1 and TRP levels in 7-d-old flies. The TRP blot is reprobed with an antibody to IPP as a loading control. Sk2 overexpression is also seen in blots probed with an Sk2 antibody. (C) A 65–70% reduction in Rh1 level and a 60% reduction in TRP level are observed in Sk2 overexpressors compared with w^{1118}. (D) Graph shows the extent of Sk2 overexpression compared with w^{1118}. (E) Photoreceptors expressing Sk2 at 30°C degenerate, whereas those at 18°C expressing $Gal80^{ts}$ do not degenerate. (F) TRP level is reduced at 30°C compared with 18°C. Sk2 overexpressor (Sk2 OE) represents GMR-Gal4–driven Sk2 at 25°C. The middle blot shows Sk2 overexpression, and the bottom blot shows loading controls. (G and H) Quantitation of TRP bands (G) and Sk2 (H) at permissive and nonpermissive temperature, and Sk2 overexpression at 25°C. $n = 3$; bars denote standard deviation.

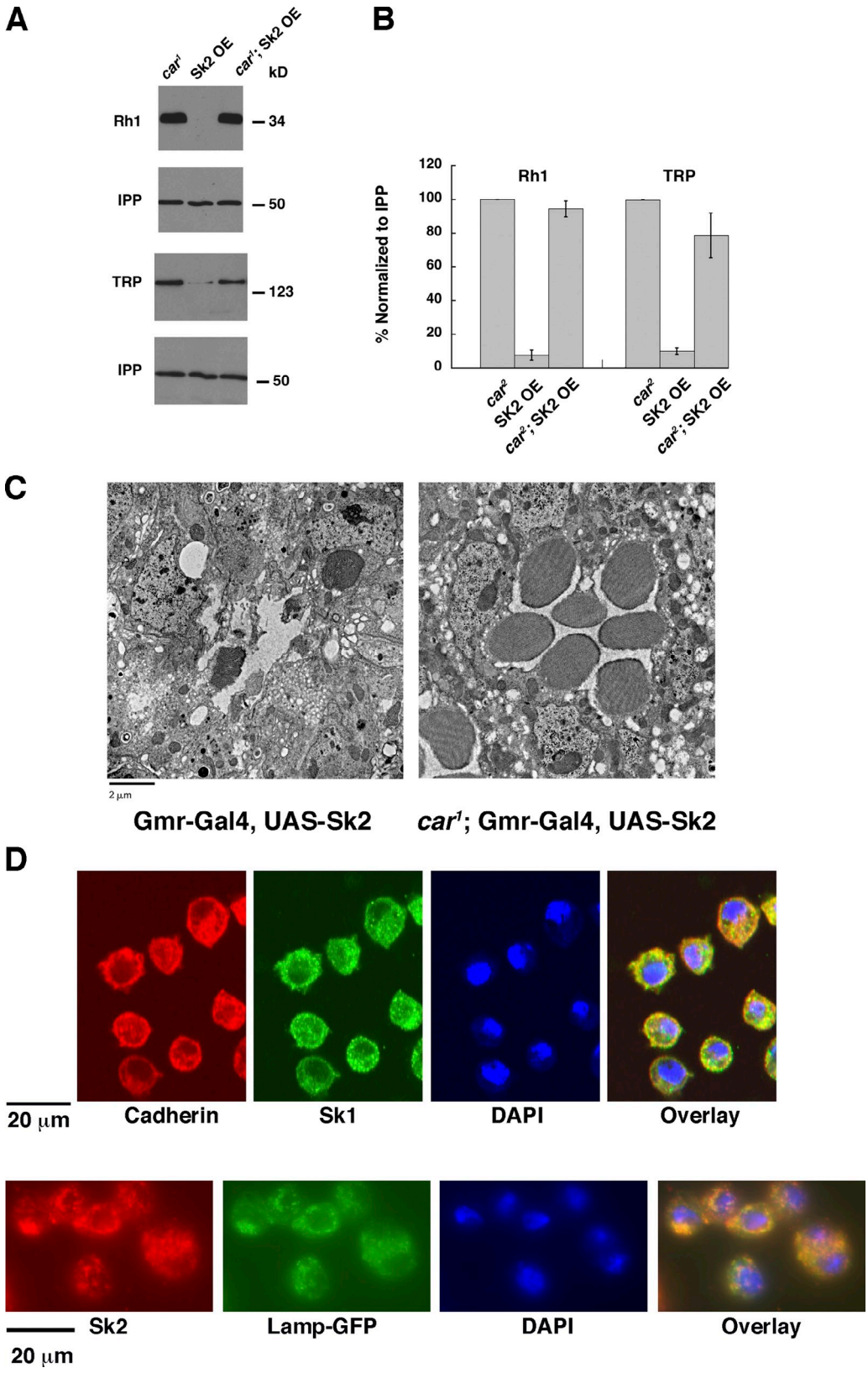

Figure 2. **Overexpression of Sk2 in a *car*[1] mutant restores Rh1 and TRP levels, and photoreceptor degeneration is suppressed.** (A) Rh1 and TRP levels are recovered when Sk2 is overexpressed in a *car* mutant. (B) The percentage of expression of Rh1 and TRP in an Sk2 overexpressor (Sk2 OE) and an Sk2 overexpressor in a *car* mutant background compared with *car* mutant alone. $n = 3$; bars denote standard deviation. (C) Degeneration is suppressed in 7-d-old photoreceptors of the Sk2 overexpressor in a *car* mutant. 4% of rhabdomeres are intact in Sk2 overexpressors, whereas 88% are intact in Sk2 overexpressors in *car*. (D) S2 cells were stained with antibodies to Sk1 and cadherin, a plasma membrane marker. Overlay shows the colocalization of Sk1 with cadherin. S2 cells constitutively expressing GFP-tagged Lamp1 were stained with antibodies to Sk2. Overlay shows the colocalization of Sk2 with Lamp1-GFP.

overexpressors shows Rh1 and TRP staining in the rhabdomeres similar to control, suggesting that they are transported to the plasma membrane (Fig. S1 D). Moreover, although the level is low, a fully mature form of Rh1 is detected on blots in Sk2 overexpressors. Because GMR-Gal4 expression begins at the third instar larval stage in differentiating photoreceptor cells, it is possible that Sk2 overexpression affects photoreceptor development, leading to low Rh1 and TRP levels. To circumvent this, we used GMR-Gal4 expression in conjunction with $Gal80^{ts}$. We raised flies at a permissive temperature at which Gal80 inhibits Gal4 transcription and, 2 d after eclosion, moved the flies to a nonpermissive temperature at which Gal80 is inhibited and allows for Gal4-mediated Sk2 expression. Photoreceptors of Sk2 overexpressors moved to a nonpermissive temperature degenerate, whereas those maintained at the permissive temperature do not undergo degeneration. This shows that targeted overeexpression of Sk2 could induce degeneration after the development of photoreceptors (Fig. 1 E). This is also accompanied by a reduction in TRP level (Fig. 1, F–H). The level of Rh1 could not be followed by this method because its expression in control flies increased during the low to high temperature shift. Therefore, we followed Rh1 expression after induction of Sk2 expression in adult flies with a heat shock Gal4 line. The Rh1 level significantly decreases by the third day after heat shock (Fig. S2 B).

In wild-type photoreceptors, Rh1 and TRP have been identified in multivesicular endosomes/bodies, which sort endocytosed membrane proteins for recycling or to lysosomes for degradation (Satoh et al., 2005). To assess whether TRP and Rh1 levels are low in Sk2 overexpressors because of enhanced degradation, we inhibited the lysosomal pathway, a main route for membrane protein degradation. We expressed Sk2 in a carnation (car) mutant background. The car gene product is the *Drosophila* homologue of VPS33A, which is part of the class C vacuolar protein sorting complex (Banta et al., 1990; Sevrioukov et al., 1999). In *Drosophila*, Car is required for the delivery of different cargo to lysosomes; in a *car* mutant, endocytosed ligands pass through early endosomes and accumulate in a Rab7-positive late endocytic compartment (Sevrioukov et al., 1999; Sriram et al., 2003; Akbar et al., 2009). Thus, *car* mutants inhibit the delivery of membrane proteins to lysosomes. When Sk2 is expressed in a *car* mutant, TRP and Rh1 levels are recovered, suggesting delivery of TRP and Rh1 to lysosomes, and their consequent degradation is inhibited (Fig. 2, A and B). Restoring TRP and Rh1 levels also suppresses degeneration (Fig. 2 C). Car is also required for the fusion of autophagosomes with lysosomes (Akbar et al., 2009). To test whether inhibition of this pathway could rescue degeneration, we inhibited the autophagic response in Sk2 overexpressors. In *Drosophila*, it has been shown that Atg1 is essential for autophagy, and expression of a dominant-negative kinase-defective Atg1 can inhibit the process (Scott et al., 2007). Coexpression of dominant-negative Atg1 in Sk2 overexpressors does not prevent photoreceptor degeneration (Fig. S2 C) and is accompanied by a decrease in Rh1 and TRP levels (not depicted). These experiments suggest that the Sk2 overexpression phenotype is not affected by altering the autophagic response by manipulating Atg1. These studies in the *car* mutant background show that TRP and Rh1 are low in Sk2 overexpressors as a result of enhanced lysosomal degradation, and inhibition of endosomal to lysosomal fusion in a *car* mutant perhaps slows down upstream events in the pathway enabling the recovery of Rh1 and TRP.

To understand why targeted expression of Sk2 leads to degeneration compared with Sk1, we tested whether the two enzymes had distinct subcellular localization patterns. We performed immunolocalization experiments in Schneider (S2) cells. In addition to cytosolic staining, Sk1 localizes to the plasma membrane, as seen by its colocalization with cadherin, a plasma membrane marker (Fig. 2 D). Sk2 shows cytoplasmic staining; additionally, we found that Sk2 can localize to lysosomal membranes, as seen by its colocalization with GFP-tagged *Drosophila* lysosome-associated membrane protein 1 (Lamp1), a lysosomal marker (Elwell and Engel, 2005). Noncolocalization experiments with markers for other organelles are shown in Fig. S3. The lysosomal localization of Sk2 could explain, in part, the accelerated degradation of Rh1 and TRP upon its overexpression, suggesting that Sk2 could influence lysosomal degradation of proteins.

Alteration in the ratio of DHS1P to S1P leads to retinal degeneration in Sk2 overexpressors and wild-type photoreceptors

As previously mentioned in this paper, Sk's phosphorylate sphingosine and DHS to S1P and DHS1P, respectively. Could any of these metabolites mediate the enhanced degradation of Rh1 and TRP and cause photoreceptor degeneration? We examined this possibility by feeding wild-type control flies (w^{1118}) with either sphingosine, DHS, S1P, or DHS1P. We custom synthesized the tetradecasphinganine (the predominant sphingoid base in *Drosophila*) version of each of these lipids. It has been shown that lethality of *lace* alleles deficient in the de novo biosynthesis of sphingolipids can be rescued when flies are raised in food supplemented with sphingosine (Adachi-Yamada et al., 1999). The lace gene encodes the LCB2 subunit of serine palmitoyltransferase, the first and rate-limiting enzyme in sphingolipid biosynthesis. We tested the efficacy of the synthesized lipids by raising *lace* heterozygotes in food containing S1P, DHS, or DHS1P. Similar to sphingosine feeding, each of the three lipids could rescue lace lethality. Rescue with sphingosine, S1P, and DHS was almost complete with Mendelian segregation of the progeny, whereas rescue with DHS1P was partial (40% of the expected number of homozygous flies eclosed in *lace* heterozygotes fed DHS1P compared with control). Using the rescue of lethality as evidence for the functionality of these lipids, we raised w^{1118} in food supplemented with each of these lipids, and photoreceptors were processed by electron microscopy. Photoreceptors of w^{1118} raised in DHS1P show degeneration, whereas those fed sphingosine, DHS, or S1P do not show significant differences (Fig. 3 A). Degeneration is accompanied by a decrease in steady-state levels of Rh1 and TRP in w^{1118} fed DHS1P compared with other flies (Fig. 3, B and C). We observed that DHS-fed flies also show some decrease in Rh1, perhaps because it can be converted to DHS1P (Fig. 3, B and C).

To assess whether the DHS1P level was altered in Sk2 overexpressors, we measured levels of sphingosine, S1P, DHS,

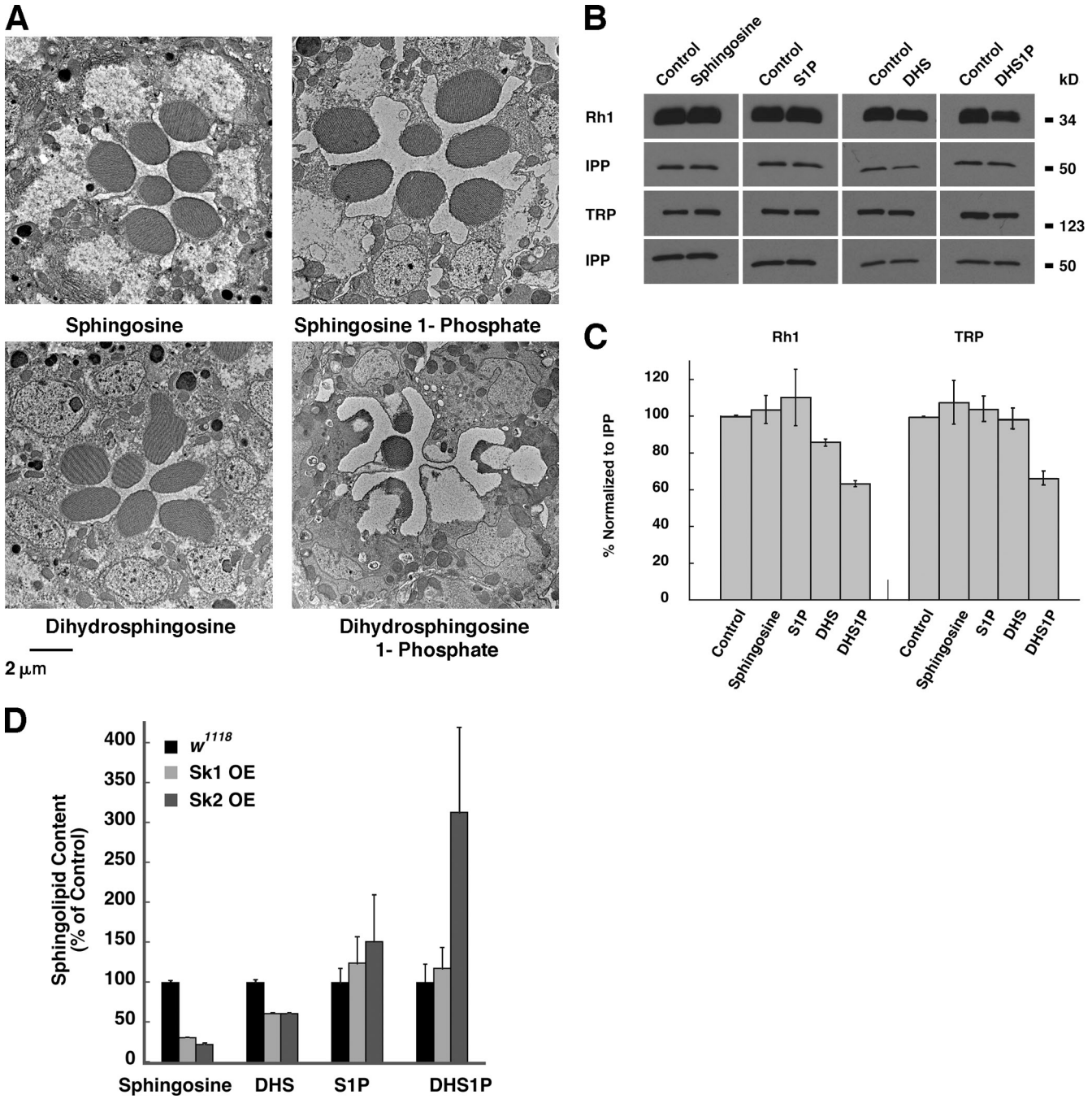

Figure 3. **Increase in DHS1P leads to retinal degeneration in w^{1118} photoreceptors accompanied by a decrease in Rh1 and TRP levels, and Sk2 overexpression increases the DHS1P level.** (A) Transmission electron micrograph of photoreceptors of w^{1118} fed sphingosine, S1P, DHS, and DHS1P. 100% of rhabdomeres are intact in w^{1118} fed sphingosine and S1P, 90% of rhabdomeres are intact in DHS-fed flies, and 27% are intact in DHS1P-fed flies. (B) Rh1 and TRP are reduced in flies fed DHS1P compared with solvent and flies fed with other lipids. (C) Rh1 and TRP levels are reduced by 40% in w^{1118} flies fed DHS1P compared with solvent. Bars denote standard deviation; $n = 3$. (D) UFLC MS/MS measurements show that Sk2 overexpressors have a higher level of DHS1P compared with control or Sk1 overexpressors. Bars denote standard error; $n = 3$.

and DHS1P in these overexpressors by ultrafast liquid chromatography coupled to tandem mass spectrometry (UFLC MS/MS). To detect endogenous DHS and DHS1P, substantial amounts of head extract were necessary. 4,000 crosses were set up for each overexpression, heads were cut, and sphingolipid-enriched fractions were prepared for mass spectrometry. Sk1 and Sk2 use both sphingosine and DHS as substrates and generate S1P and DHS1P. However, Sk2 overexpressors preferentially accumulate DHS1P compared with Sk1 (Fig. 3 D). Thus, the ratio of DHS1P to S1P is increased in Sk2 overexpressors, whereas that in Sk1 is comparable with w^{1118}. Results from feeding experiments and mass spectrometric measurements in Sk2 overexpressors show that an increase in DHS1P over S1P correlates with photoreceptor degeneration and lysosomal degradation of Rh1 and TRP.

Based on these results, we tested whether Sk1 photoreceptors could be induced to degenerate by raising Sk1 overexpressors

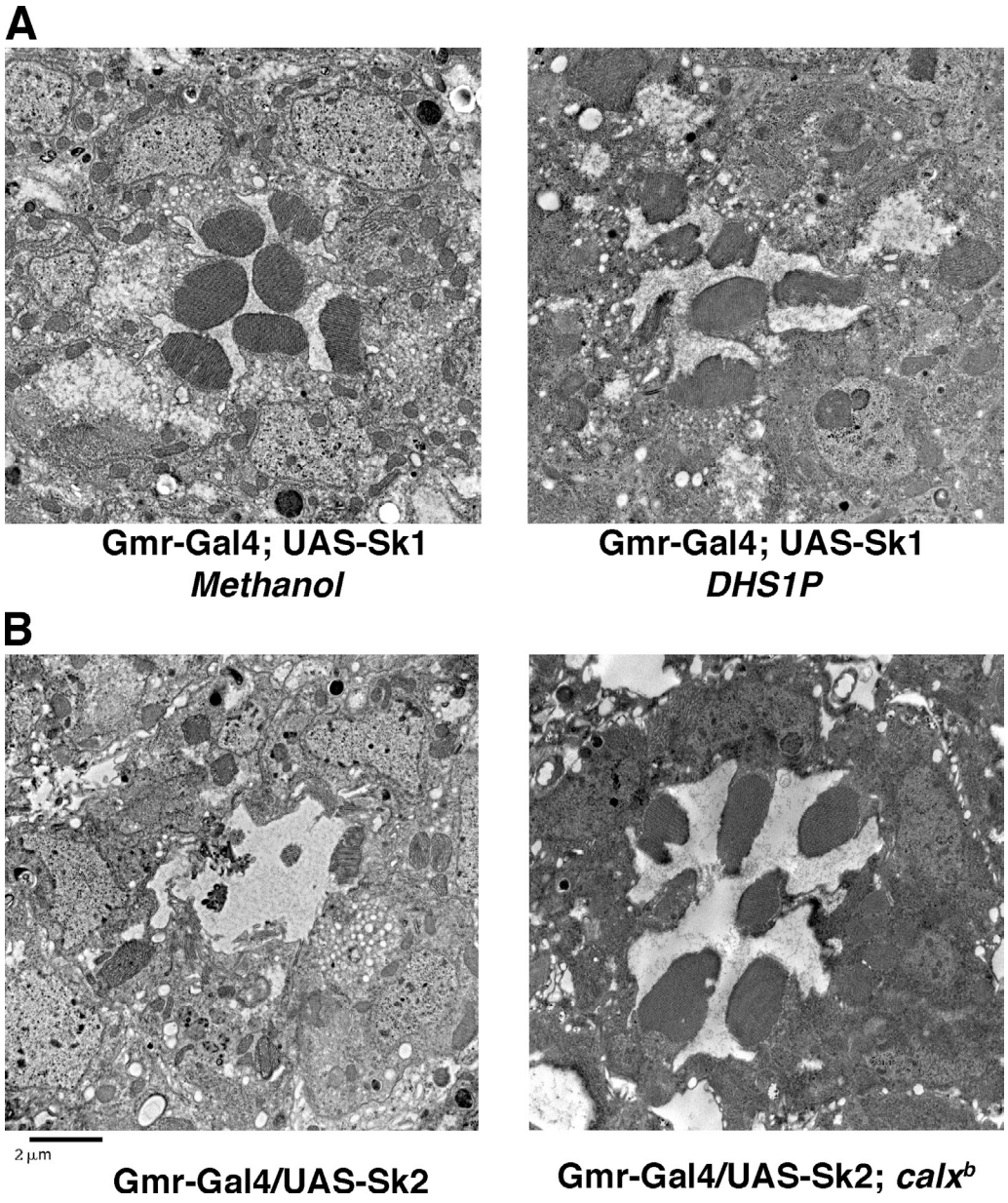

Figure 4. **Increasing DHS1P induces Sk1-expressing photoreceptors to degenerate, and photoreceptor degeneration in Sk2 overexpressors is suppressed in a CalX mutant.** (A) Photoreceptors of Sk1 overexpressors degenerate when DHS1P is increased. In DHS1P-fed Sk1 flies, 32% of the rhabdomeres are intact compared with flies raised in solvent. (B) Photoreceptor degeneration in 7-d-old Sk2 overexpressors is suppressed in a $calx^B$ mutant, suggesting altered calcium homeostasis is a likely cause of degeneration. 81% of the rhabdomeres are intact in Sk2 overexpressors in $calx^B$; however, many rhabdomeres are elongated in shape.

in DHS1P-containing food. Indeed, DHS1P-fed Sk1 overexpressors degenerate compared with vehicle-fed flies (Fig. 4 A). Several molecular mechanisms have been proposed for retinal degeneration in *Drosophila* photoreceptors (Wang and Montell, 2007). One of the reasons why photoreceptors degenerate is because of an insufficient or excess amount of Ca^{2+} in the cells. In *rdgA*, TRP channels are constitutively active, and this mutant degenerates because of an uncontrolled calcium influx into photoreceptors, whereas degeneration in *trp* and *inaF* is caused by an insufficient Ca^{2+} influx (Li et al., 1999; Raghu et al., 2000). Several of these mutants are subject to epistatic interaction and, thus, comprise components of specific genetic pathways. To examine whether Sk and its metabolites play a role in these pathways, we examined the effect of Sk2 overexpression in many phototransduction mutant backgrounds. Experiments with *arr2*, *ninaE*, *inaC*, *ninaC*, and *trp* mutants show that they do not suppress degeneration observed in Sk2 overexpressors (unpublished data). However, mutants in CalX partially suppress the degeneration (Fig. 4 B). In *Drosophila* photoreceptors, Ca^{2+} entry is critical for the activation and subsequent attenuation of signaling (O'Tousa, 2002). To accomplish dynamic changes in Ca^{2+} levels, a calcium extrusion mechanism mediated by Na^+/Ca^{2+} exchangers counters TRP-dependent Ca^{2+} influx in cells. CalX is one such exchanger, and the *calx* mutant shows a transient response to light, a defect in signal amplification, and an increase in intracellular Ca^{2+} concentration (Wang et al., 2005).

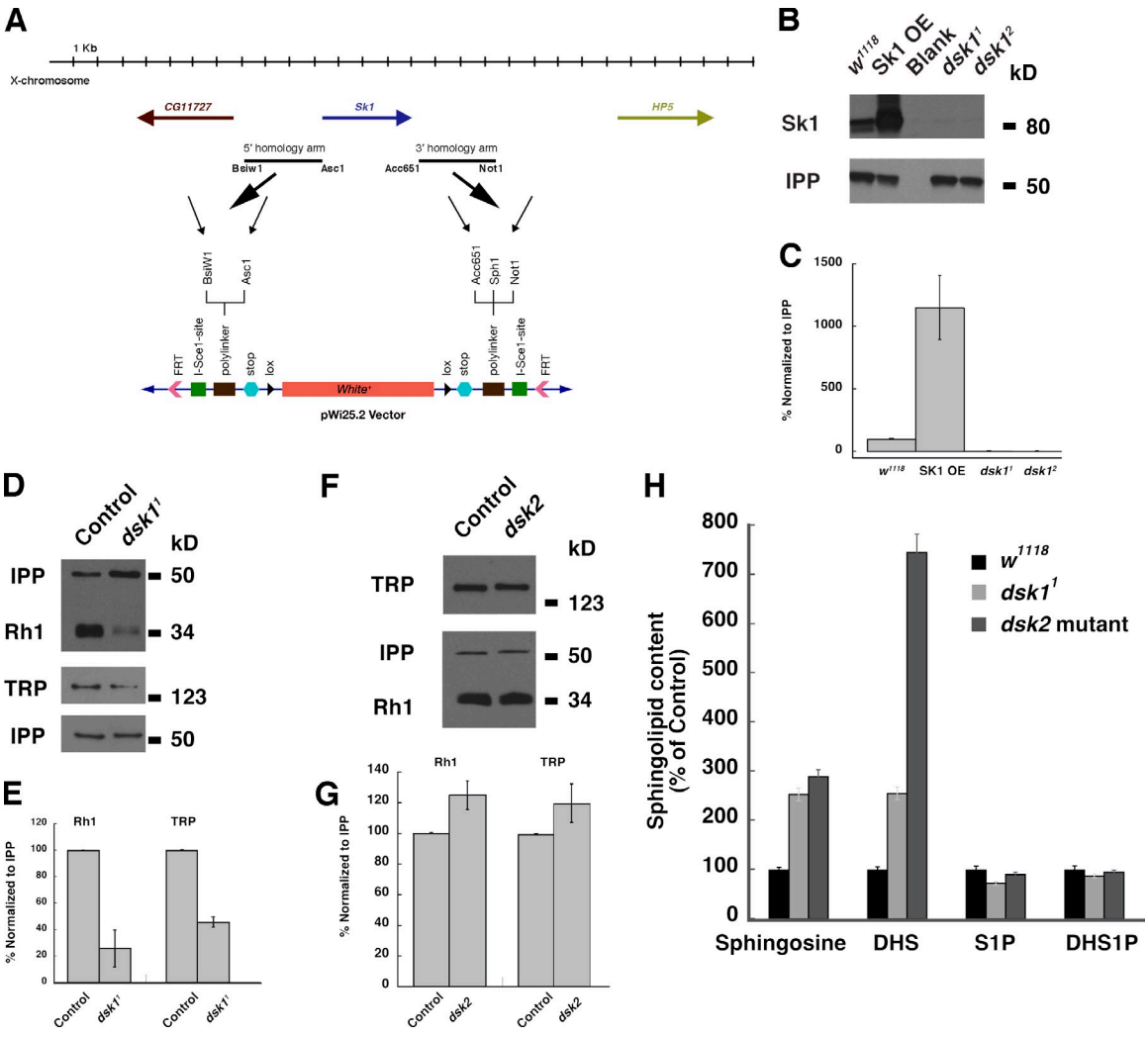

Figure 5. **Altered DHS1P to S1P ratio in Sk1 mutants.** (A) The targeting vector used to generate Sk1 mutants by ends-out homologous recombination. (B) *sk1* mutants do not show Sk1 protein, indicating that they are null mutants. (C) Quantification of Sk1 in overexpressors and *sk1* mutant alleles. (D) Rh1 and TRP are low in 1-d-old *sk1*^{1} compared with control *cinnabar.brown* (*cn.bw*) flies. (E) Quantification of Rh1 and TRP shows that Rh1 is decreased to 30% and TRP to 40% in *sk1* mutants compared with control *cn.bw* flies. (F) Rh1 and TRP in *sk2* compared with control flies. (G) Quantification of Rh1 and TRP bands in *sk2*. (C, E, and G) $n = 3$; bars denote standard deviation. (H) Mass spectrometric measurements show a 20% reduction in S1P level in *sk1*. $n = 3$; bars denote standard error. OE, overexpressor.

Because the CalX mutant suppresses degeneration in Sk2 overexpressors, we reason that calcium homeostasis is disturbed in these flies.

Sk1 mutant shows trafficking defects and an altered DHS1P/S1P ratio

To determine whether endogenous Sk proteins modulate Rh1 and TRP trafficking by regulating DHS1P and S1P levels, we decided to analyze Sk1 and Sk2 mutants. A *P*-element mutant in Sk2 has been previously characterized; these mutant flies are viable and show impaired flight performance and diminished ovulation (Herr et al., 2004). Because Sk1 mutants were not available, we used ends-out homologous recombination–based gene targeting to generate Sk1-null mutant flies (Gong and Golic, 2003). The design of the targeting vector is shown in Fig. 5 A. A total of 1,500 lines were set up in the screen, and we recovered three independent targeting events wherein the endogenous gene was replaced with the deletion construct. Sk1 protein could not be detected by Western analysis in these deletion lines (Fig. 5, B and C). Sk1 mutant flies are viable and fertile at room temperature with no external morphological defects. We looked at the steady-state levels of TRP and Rh1 levels in *sk1* and *sk2*. 1-d-old *sk1* flies show low Rh1 and TRP. *sk2* flies do not show considerable differences in their levels (Fig. 5, D–G). To test whether these mutants show alterations in their substrate or product metabolites, lipid fractions were subjected to UFLC MS/MS. As shown in Fig. 5 H, both *sk1* and *sk2* accumulate sphingosine and DHS. The ratio of DHS1P to S1P is increased in the Sk1 mutant because of the reduction in S1P level as compared with Sk2 mutant and control flies. The Sk2 *P*-element mutant reported earlier is a hypomorph and not a null mutant because we could detect a transcript and a small amount of protein (unpublished data). The metabolite differences are not dramatic in the mutants as in the overexpressors because of the redundancy of the Sk1 and Sk2 function. This is also reflected in the observation that although single mutants are viable, Sk1

and Sk2 double mutants are lethal (unpublished data). In SphK1$^{-/-}$ mice, S1P tissue levels are normal, indicating that SphK deficiency could be compensated for by SphK2 (Allende et al., 2004). Only SphK1$^{-/-}$ and SphK2$^{-/-}$ double knockout has no measurable S1P levels (Mizugishi et al., 2005). It is also relevant to consider that S1P levels are likely regulated by the degrading enzymes, S1P lyase, and phosphatases.

Although S1P has been well studied, less is known about the effects of DHS1P. An elevated level of DHS1P has an antiproliferative effect in yeast (Kim et al., 2000). Recent experiments in mammalian cells show opposite effects of DHS1P and S1P on transforming growth factor β/Smad signaling (Bu et al., 2006). Despite being closely related enzymes, mouse SPhK1 and SPhK2 have opposite effects on cell survival: SPhK1 is antiapoptotic, whereas SPhK2 promotes apoptosis (Maceyka et al., 2005). Similar to mammalian cells, our observations in *Drosophila* support the idea that although the two kinases have some redundant functions, they can localize to distinct cellular compartments, and localized production of their metabolites could cause distinct changes in the lipid microenvironment that either alter the structure of cargo molecules or alter their behavior to trigger differential turnover. Although we have studied Rh1 and TRP using photoreceptors as a model, it is reasonable to hypothesize that these metabolites would similarly affect the endolysosomal trafficking of other membrane proteins. Addressing how these lipids interact with other lipids and protein families involved in trafficking and sorting will improve our understanding of the participation of lipids in endolysosomal homeostasis.

Materials and methods

Fly stocks and husbandry

Drosophila stocks were raised on standard maize meal agar and maintained at 25°C unless otherwise mentioned. *Sk2*^{KG05894}, *car*^{1}, *calx*^{B}, and *lace*^{k05305} were obtained from the Bloomington Stock Center. Upstream activating sequence (UAS)–Sk2 flies expressing Gal80^{ts} and control flies were generated at 18°C and shifted at the adult stage after 1 d to 30°C. For heat shock experiments, Sk2 transgenics were crossed to Gal4-hsp70, and adult flies were heat shocked at 37°C. Atg1^{K38Q} flies (Scott et al., 2007) were obtained from E. Baehrecke (University of Massachusetts Medical School, Worcester, MA). Sk1 cDNA (EST RE64552) was cloned into the pUAST vector as a Kpn1–Not1 fragment, whereas Sk2 cDNA (LD112747) was cloned as an EcoR1–Xba1 fragment. These constructs were injected into *w*^{1118} embryos using standard techniques to generate transgenic flies. Multiple amino acid mutations of full-length Sk2 (*pUAS-Sk2*) were prepared using a site-directed mutagenesis kit (Quick Change XL; Agilent Technologies). The mutagenic oligonucleotide used to generate the mutant construct was Sk2$^{GSGN312–315DDDD}$ (5′-CATTCCTTGCGACGACGACGACGGATTGGCCCGC-3′; substituted nucleotides are underlined). The mutant was sequenced, and the pUAST construct was injected into *w*^{1118} embryos to generate transgenic flies.

Generation of antibodies to Sk1 and Sk2

Sk1 full-length cDNA was cloned as a Not1–Sal1 fragment into pGEX4T3. Full-length protein was expressed, ran on gels, electroeluted, and used for the injection of rabbits. Antiserum was affinity purified by incubating it with full-length protein transferred to a nitrocellulose membrane. Sk2 was cloned as two fragments—N terminal (1.2 kb) and C terminal (1.2 kb)—into pmalc2×. Each fragment was expressed and purified, and the two purified fragments were mixed and injected into rabbits. Antiserum was affinity purified as previously described.

Genetic screen to isolate Sk1-null mutants

The Sk1 knockout flies (*sk1*^{1} and *sk1*^{2}) were generated by ends-out homologous recombination (Gong and Golic, 2003). The targeting vector was designed to delete the entire Sk1 open reading frame, including 222 bp upstream of the start codon and 454 bp downstream of the stop codon. A 3,081-bp genomic fragment (extending from −3,103 to −222 of the start codon) was inserted into the BsiW1–Asc1 site of the vector as the upstream homology arm, and another 3.0-kb genomic fragment (454–3,453) was inserted into the Acc651–Not1 site of the pw25.2 vector. The targeting construct was injected into *w*^{1118} embryos, and six transformants were selected on the basis of eye pigmentation. Flies carrying the targeting construct on the X chromosome were crossed to *w*;[V^{+}.70ISceI]2B[ry^{+}, 70FLP] flies, and the resulting mosaic flies were crossed to P{hs-I-CreI.R}2A, v[1];ry[506] flies. The resulting red-eyed progeny were screened by Western analysis for loss of Sk1 protein, and three independent targeted alleles were recovered.

Electron microscopy

For all electron microscopic experiments, unless otherwise specified, 7-d-old flies grown at 25°C were decapitated under anesthesia, and their heads were dissected, fixed, and processed as previously described (Acharya et al., 2003).

Immunohistochemistry

Drosophila Sk1 (as a Kpn1–Not1 fragment) and Sk2 (as a Kpn1–EcoR1 fragment) were cloned into pMTV5 HisA, and stable S2 cells expressing Sk1 and Sk2 were generated. Sk1 staining was performed on S2 cells, whereas Sk2 staining was performed on S2 cells constitutively expressing GFP-tagged *Drosophila* Lamp1 under the control of an actin promoter. S2 cells were stained as described previously (Acharya et al., 2008; Dasgupta et al., 2009). In brief, S2 cells on poly-lysine–coated coverslips were fixed with 4% paraformaldehyde and blocked in PBS containing 0.2% Triton X-100 and 5% BSA for 2 h. The cells were stained with primary antibody in blocking buffer overnight at 4°C, washed with PBS, and stained with secondary antibody for 1 h at room temperature. Cells were washed, and coverslips were mounted using Vectashield (Vector Laboratories). Immunofluorescent staining of adult eyes was performed following protocols described previously (Walther and Pichaud, 2007). Retinae were dissected in 4% paraformaldehyde and blocked in 10% normal goat serum in PBS supplemented with 0.3% Triton X-100. Eyes were incubated overnight at 4°C with primary antibody in blocking solution. The eyes were washed and incubated in secondary antibody at room temperature for 2–4 h. Samples were washed extensively and mounted using Vectashield. S2 cells expressing Lamp1-GFP were a gift from R. Vale and J. Engel (University of California, San Francisco, San Francisco, CA). The antibody to Lavalamp was a gift from J. Sisson (University of Texas, Austin, TX). Affinity-purified goat polyclonal antibody to cadherin was obtained from Santa Cruz Biotechnology, Inc., rabbit polyclonal antibody to Rab5 was obtained from Abcam, and mouse monoclonal antibody to V5 was obtained from Invitrogen. The Rhodopsin monoclonal antibody (4C5) and TRP monoclonal antibody (83F6) were obtained from the Developmental Studies Hybridoma Bank under the auspices of the National Institute of Child Health and Human Development and maintained by the University of Iowa's Department of Biological Sciences. The antibodies were used at the following dilutions: Sk1 at 1:5, Sk2 at 1:10, V5 at 1:750, cadherin at 1:25, Lavalamp at 1:1,000, Rab 5 at 1:500, Rh1 at 1:500, and TRP at 1:100. Secondary antibodies were used at 1:1,500 dilutions. For the biotinylation experiments, biotinylated affinity-purified anti–rabbit IgG, fluorescein-conjugated streptavidin, and the blocking kit were obtained from Vector Laboratories. Whole-mount retinae were viewed on a spinning-disk confocal microscope (Solamere Technology Group–modified CSU10; Yokogawa). For the immunolocalization of Sk1, images were acquired on a confocal microscope (LSM 510; Carl Zeiss, Inc.) using a 40× objective. For localization of Sk2, stained sections were visualized with a 100× objective using an imaging system (Axioplan; Carl Zeiss, Inc.) using a camera (ORCA-ER; Hamamatsu) and Axiovision 4.5 software (Carl Zeiss, Inc.).

Western analysis

Fly heads were dissected from 7-d-old flies (unless otherwise specified), homogenized in sample buffer, boiled, and subjected to SDS-PAGE and Western analysis. For detection of Rh1 and TRP, the samples were incubated at 37°C for 40 min and then subjected to SDS-PAGE and Western blotting. Antibodies to Arr2, InaD, Gα, and inositol polyphosphate 1 phosphatase (IPP) were gifts from C. Zuker (Columbia University, New York, NY), and antibody to NinaC was a gift from C. Montell (Johns Hopkins University, Baltimore, MD).

Feeding of sphingolipids to flies

Tetradecasphingosine (long-chain base of 14-carbon length) was obtained from Matreya. DHS, DHS1P, and S1P with a 14-carbon long-chain base

were custom synthesized at the Lipidomics Synthetic Core (A. Bielawska and Z. Szulc, Medical University of South Carolina, Charleston, SC). Sphingosine and DHS were fed at a final concentration of 300 µM, whereas their phosphates were fed at 150 µM. Standard fly food containing 20 parent w^{1118} flies (10 males and 10 females at 1–2 d old) was supplemented with each of these sphingolipids, and flies were raised at 25°C. The control vials contained food supplemented with either methanol (used for dissolving S1P and DHS1P) or ethanol (used for dissolving sphingosine and DHS). *Lace* heterozygotes were used as a positive control in all feeding experiments. Newly eclosed flies were aged for different days in sphingolipid-containing food and fixed, and their eyes were processed by electron microscopy.

Estimation of sphingolipids by mass spectrometry

The mass spectrometric standard mix was obtained from Avanti Polar Lipids, Inc. Sphingolipid-enriched fractions were prepared from head extracts of 1,000 flies for each condition following the protocol described in Merrill et al. (2005). Frozen fly heads were homogenized in 500 µl methanol/chloroform (2:1) using a Teflon homogenizer in a microcentrifuge tube. The homogenate was transferred to a glass tube, and 1.5 ml methanol/chloroform (2:1) was added followed by 500 µl of water and vortexed. The homogenate was sonicated in a water bath–type sonicator for 20 min and incubated overnight at 37°C. To the extract, 1 ml of water and 500 µl chloroform were added, vortexed, and centrifuged at 1,000 rpm for 10 min at room temperature. The organic phase was collected and dried under nitrogen. Extracts were redissolved in 2 ml synthetic upper (methanol/water/chloroform, 94:96:6) and applied to a pretreated SepPak C18 column for solid-phase extraction (Waters Corporation). The column was washed with 4 ml of water, and lipids were extracted in 4 ml methanol followed by 4 ml methanol/chloroform. The samples were dried under nitrogen and redissolved in the requisite amount of chloroform/methanol (1:1). For sphingolipid analyses, liquid chromatography was performed on the Prominence $UFLC_{XR}$ system (Shimadzu Co.). Separation was achieved on an ACQUITY UPLC HSS T3 column (100 × 2.1–mm internal diameter) maintained at 60°C. The mobile phase was composed of 5-mM $HCOONH_4$ in H_2O containing 0.1% HCOOH and 5-mM phosphoric acid (solvent A) and 5-mM $HCOONH_4$ in MeOH containing 0.1% HCOOH and 5-µM phosphoric acid (solvent B) with a flow rate of 400 µl/min. The column was eluted with a linear gradient elution from 25 to 99% of solvent B for 9 min and then with isocratic elution with 99% of solvent B for 3 min. The column temperature was at 60°C. Mass spectrometric detection was performed on a mass spectrometer (AB SCIEX QTRAP 5500; AB SCIEX Japan, Ltd.) with an electrospray ionization source set in both positive and negative modes. Quantification was performed with a scan time of 50 ms per transition with the following selected reaction monitoring: sphingosine d14:1 (244.2/196.2), d16:1 (272.2/224.2), and d17:1 (286.2/238.2); DHS d14:1 (246.2/198.2), d16:1 (274.2/226.2), and d17:1 (288.2/240.2); S1P d14:1 (322.2/78.8), d16:1 (350.2/78.8), and d17:1 (364.2/78.8); and DHS1P d14:1 (324.2/78.8), d16:1 (352.2/78.8), and d17:1 (366.2/78.8), with d being the number of carbon atoms in the long-chain base of each sphingolipid. The values for the mammalian fibroblasts are sphingosine d18 (300.2/252.2); DHS (302.2/254.2); S1P (378.2/78.8); and DHS1P (380.2/78.8). The following parameters were used in this study: ion spray voltages of 5,500 V (positive) and −4,500 V (negative), a source temperature of 350°C, ion spray nebulizer gas of 50 psi, turbo ion spray heater gas of 70 psi, and curtain gas of 10 psi. The optimized declustering potential was 60 for sphingosine and DHS, whereas it was −150 for their phosphates. The collision energy was 26 for sphingosine and DHS and −68 for their phosphates. The entrance potential was 10 for sphingosine and DHS and −10 for their phosphates. The collision cell exit potential for sphingosine and DHS was 15 and −13 for their phosphates. The peak area of the sample was divided by the peak area of the standard in each case.

Online supplemental material

Fig. S1 shows that both sphingosine kinases are expressed in the retina, and overexpression of an inactive Sk2 does not result in photoreceptor degeneration. Fig. S2 shows that steady-state levels of some of the phototransduction components are not significantly affected in Sk2 overexpressors, and overexpression of a dominant-negative ATG1 does not suppress Sk2 degeneration. Fig. S3 shows noncolocalization of Sk1 and Sk2 with early endosomal and Golgi markers. Online supplemental material is available at http://www.jcb.org/cgi/content/full/jcb.201004098/DC1.

We are grateful to Drs. Zdzislaw Szulc and Alicja Bielawska for the synthesis of sphingolipids. We thank Ms. Kayoko Hagiwara (AB SCIEX Japan, Ltd) for discussions and support with mass spectrometry. We thank Drs. Charles Zuker, Craig Montell, John Sisson, Ron Vale, and Joanne Engel for gifts of reagents. We thank Drs. Kartik Venkatachalam and Craig Montell for helpful discussions. We thank Kathya Acharya for help with figures.

This work is supported by a National Institutes of Health grant (RO1EY16469) to U. Acharya and by the intramural division of the National Cancer Institute to J.K. Acharya.

Submitted: 20 April 2010
Accepted: 14 January 2011

References

Acharya, J.K., U. Dasgupta, S.S. Rawat, C. Yuan, P.D. Sanxaridis, I. Yonamine, P. Karim, K. Nagashima, M.H. Brodsky, S. Tsunoda, and U. Acharya. 2008. Cell-nonautonomous function of ceramidase in photoreceptor homeostasis. *Neuron.* 57:69–79. doi:10.1016/j.neuron.2007.10.041

Acharya, U., and J.K. Acharya. 2005. Enzymes of sphingolipid metabolism in *Drosophila melanogaster*. *Cell. Mol. Life Sci.* 62:128–142. doi:10.1007/s00018-004-4254-1

Acharya, U., S. Patel, E. Koundakjian, K. Nagashima, X. Han, and J.K. Acharya. 2003. Modulating sphingolipid biosynthetic pathway rescues photoreceptor degeneration. *Science.* 299:1740–1743. doi:10.1126/science.1080549

Acharya, U., M.B. Mowen, K. Nagashima, and J.K. Acharya. 2004. Ceramidase expression facilitates membrane turnover and endocytosis of rhodopsin in photoreceptors. *Proc. Natl. Acad. Sci. USA.* 101:1922–1926. doi:10.1073/pnas.0308693100

Adachi-Yamada, T., T. Gotoh, I. Sugimura, M. Tateno, Y. Nishida, T. Onuki, and H. Date. 1999. De novo synthesis of sphingolipids is required for cell survival by down-regulating c-Jun N-terminal kinase in *Drosophila* imaginal discs. *Mol. Cell. Biol.* 19:7276–7286.

Akbar, M.A., S. Ray, and H. Krämer. 2009. The SM protein Car/Vps33A regulates SNARE-mediated trafficking to lysosomes and lysosome-related organelles. *Mol. Biol. Cell.* 20:1705–1714. doi:10.1091/mbc.E08-03-0282

Alemany, R., C.J. van Koppen, K. Danneberg, M. Ter Braak, and D. Meyer Zu Heringdorf. 2007. Regulation and functional roles of sphingosine kinases. *Naunyn Schmiedebergs Arch. Pharmacol.* 374:413–428. doi:10.1007/s00210-007-0132-3

Allende, M.L., T. Sasaki, H. Kawai, A. Olivera, Y. Mi, G. van Echten-Deckert, R. Hajdu, M. Rosenbach, C.A. Keohane, S. Mandala, et al. 2004. Mice deficient in sphingosine kinase 1 are rendered lymphopenic by FTY720. *J. Biol. Chem.* 279:52487–52492. doi:10.1074/jbc.M406512200

Alloway, P.G., L. Howard, and P.J. Dolph. 2000. The formation of stable rhodopsin-arrestin complexes induces apoptosis and photoreceptor cell degeneration. *Neuron.* 28:129–138. doi:10.1016/S0896-6273(00)00091-X

Bankaitis, V.A., C.J. Mousley, and G. Schaaf. 2010. The Sec14 superfamily and mechanisms for crosstalk between lipid metabolism and lipid signaling. *Trends Biochem. Sci.* 35:150–160. doi:10.1016/j.tibs.2009.10.008

Banta, L.M., T.A. Vida, P.K. Herman, and S.D. Emr. 1990. Characterization of yeast Vps33p, a protein required for vacuolar protein sorting and vacuole biogenesis. *Mol. Cell. Biol.* 10:4638–4649.

Baron, C.L., and V. Malhotra. 2002. Role of diacylglycerol in PKD recruitment to the TGN and protein transport to the plasma membrane. *Science.* 295:325–328. doi:10.1126/science.1066759

Birkeland, H.C., and H. Stenmark. 2004. Protein targeting to endosomes and phagosomes via FYVE and PX domains. *Curr. Top. Microbiol. Immunol.* 282:89–115.

Bu, S., M. Yamanaka, H. Pei, A. Bielawska, J. Bielawski, Y.A. Hannun, L. Obeid, and M. Trojanowska. 2006. Dihydrosphingosine 1-phosphate stimulates MMP1 gene expression via activation of ERK1/2-Ets1 pathway in human fibroblasts. *FASEB J.* 20:184–186.

Chinchore, Y., A. Mitra, and P.J. Dolph. 2009. Accumulation of rhodopsin in late endosomes triggers photoreceptor cell degeneration. *PLoS Genet.* 5:e1000377. doi:10.1371/journal.pgen.1000377

Dasgupta, U., T. Bamba, S. Chiantia, P. Karim, A.N. Tayoun, I. Yonamine, S.S. Rawat, R.P. Rao, K. Nagashima, E. Fukusaki, et al. 2009. Ceramide kinase regulates phospholipase C and phosphatidylinositol 4, 5, bisphosphate in phototransduction. *Proc. Natl. Acad. Sci. USA.* 106:20063–20068.

Dickson, R.C., C. Sumanasekera, and R.L. Lester. 2006. Functions and metabolism of sphingolipids in *Saccharomyces cerevisiae*. *Prog. Lipid Res.* 45:447–465. doi:10.1016/j.plipres.2006.03.004

Elwell, C., and J.N. Engel. 2005. *Drosophila melanogaster* S2 cells: a model system to study *Chlamydia* interaction with host cells. *Cell. Microbiol.* 7:725–739. doi:10.1111/j.1462-5822.2005.00508.x

Futerman, A.H., and H. Riezman. 2005. The ins and outs of sphingolipid synthesis. *Trends Cell Biol.* 15:312–318. doi:10.1016/j.tcb.2005.04.006

Gong, W.J., and K.G. Golic. 2003. Ends-out, or replacement, gene targeting in *Drosophila*. *Proc. Natl. Acad. Sci. USA.* 100:2556–2561. doi:10.1073/pnas.0535280100

Groux-Degroote, S., S.M. van Dijk, J. Wolthoorn, S. Neumann, A.C. Theos, A.M. De Mazière, J. Klumperman, G. van Meer, and H. Sprong. 2008. Glycolipid-dependent sorting of melanosomal from lysosomal membrane proteins by lumenal determinants. *Traffic.* 9:951–963. doi:10.1111/j.1600-0854.2008.00740.x

Gruenberg, J. 2003. Lipids in endocytic membrane transport and sorting. *Curr. Opin. Cell Biol.* 15:382–388. doi:10.1016/S0955-0674(03)00078-4

Hait, N.C., C.A. Oskeritzian, S.W. Paugh, S. Milstien, and S. Spiegel. 2006. Sphingosine kinases, sphingosine 1-phosphate, apoptosis and diseases. *Biochim. Biophys. Acta.* 1758:2016–2026. doi:10.1016/j.bbamem.2006.08.007

Hannun, Y.A., and L.M. Obeid. 2008. Principles of bioactive lipid signalling: lessons from sphingolipids. *Nat. Rev. Mol. Cell Biol.* 9:139–150. doi:10.1038/nrm2329

Hardie, R.C., and P. Raghu. 2001. Visual transduction in *Drosophila*. *Nature.* 413:186–193. doi:10.1038/35093002

Herr, D.R., H. Fyrst, M.B. Creason, V.H. Phan, J.D. Saba, and G.L. Harris. 2004. Characterization of the *Drosophila* sphingosine kinases and requirement for Sk2 in normal reproductive function. *J. Biol. Chem.* 279:12685–12694. doi:10.1074/jbc.M310647200

Kearns, B.G., T.P. McGee, P. Mayinger, A. Gedvilaite, S.E. Phillips, S. Kagiwada, and V.A. Bankaitis. 1997. Essential role for diacylglycerol in protein transport from the yeast Golgi complex. *Nature.* 387:101–105. doi:10.1038/387101a0

Kim, S., H. Fyrst, and J. Saba. 2000. Accumulation of phosphorylated sphingoid long chain bases results in cell growth inhibition in *Saccharomyces cerevisiae*. *Genetics.* 156:1519–1529.

Kiselev, A., M. Socolich, J. Vinós, R.W. Hardy, C.S. Zuker, and R. Ranganathan. 2000. A molecular pathway for light-dependent photoreceptor apoptosis in *Drosophila*. *Neuron.* 28:139–152. doi:10.1016/S0896-6273(00)00092-1

Kobayashi, T., M.H. Beuchat, J. Chevallier, A. Makino, N. Mayran, J.M. Escola, C. Lebrand, P. Cosson, T. Kobayashi, and J. Gruenberg. 2002. Separation and characterization of late endosomal membrane domains. *J. Biol. Chem.* 277:32157–32164. doi:10.1074/jbc.M202838200

Kohama, T., A. Olivera, L. Edsall, M.M. Nagiec, R. Dickson, and S. Spiegel. 1998. Molecular cloning and functional characterization of murine sphingosine kinase. *J. Biol. Chem.* 273:23722–23728. doi:10.1074/jbc.273.37.23722

Li, C., C. Geng, H.T. Leung, Y.S. Hong, L.L. Strong, S. Schneuwly, and W.L. Pak. 1999. INAF, a protein required for transient receptor potential Ca(2+) channel function. *Proc. Natl. Acad. Sci. USA.* 96:13474–13479. doi:10.1073/pnas.96.23.13474

Liu, H., M. Sugiura, V.E. Nava, L.C. Edsall, K. Kono, S. Poulton, S. Milstien, T. Kohama, and S. Spiegel. 2000. Molecular cloning and functional characterization of a novel mammalian sphingosine kinase type 2 isoform. *J. Biol. Chem.* 275:19513–19520. doi:10.1074/jbc.M002759200

Maceyka, M., H. Sankala, N.C. Hait, H. Le Stunff, H. Liu, R. Toman, C. Collier, M. Zhang, L.S. Satin, A.H. Merrill Jr., et al. 2005. SphK1 and SphK2, sphingosine kinase isoenzymes with opposing functions in sphingolipid metabolism. *J. Biol. Chem.* 280:37118–37129. doi:10.1074/jbc.M502207200

Maceyka, M., S. Milstien, and S. Spiegel. 2009. Sphingosine-1-phosphate: the Swiss army knife of sphingolipid signaling. *J. Lipid Res.* 50(Suppl):S272–S276. doi:10.1194/jlr.R800065-JLR200

Merrill, A.H. Jr., M.C. Sullards, J.C. Allegood, S. Kelly, and E. Wang. 2005. Sphingolipidomics: high-throughput, structure-specific, and quantitative analysis of sphingolipids by liquid chromatography tandem mass spectrometry. *Methods.* 36:207–224. doi:10.1016/j.ymeth.2005.01.009

Mizugishi, K., T. Yamashita, A. Olivera, G.F. Miller, S. Spiegel, and R.L. Proia. 2005. Essential role for sphingosine kinases in neural and vascular development. *Mol. Cell. Biol.* 25:11113–11121. doi:10.1128/MCB.25.24.11113-11121.2005

Mousley, C.J., K.R. Tyeryar, P. Vincent-Pope, and V.A. Bankaitis. 2007. The Sec14-superfamily and the regulatory interface between phospholipid metabolism and membrane trafficking. *Biochim. Biophys. Acta.* 1771:727–736.

Mukherjee, S., and F.R. Maxfield. 2000. Role of membrane organization and membrane domains in endocytic lipid trafficking. *Traffic.* 1:203–211. doi:10.1034/j.1600-0854.2000.010302.x

Odorizzi, G., M. Babst, and S.D. Emr. 2000. Phosphoinositide signaling and the regulation of membrane trafficking in yeast. *Trends Biochem. Sci.* 25:229–235. doi:10.1016/S0968-0004(00)01543-7

Olivera, A., and S. Spiegel. 1993. Sphingosine-1-phosphate as second messenger in cell proliferation induced by PDGF and FCS mitogens. *Nature.* 365:557–560. doi:10.1038/365557a0

Orem, N.R., L. Xia, and P.J. Dolph. 2006. An essential role for endocytosis of rhodopsin through interaction of visual arrestin with the AP-2 adaptor. *J. Cell Sci.* 119:3141–3148. doi:10.1242/jcs.03052

O'Tousa, J.E. 2002. Ca2+ regulation of *Drosophila* phototransduction. *Adv. Exp. Med. Biol.* 514:493–505.

Pichler, H., and H. Riezman. 2004. Where sterols are required for endocytosis. *Biochim. Biophys. Acta.* 1666:51–61. doi:10.1016/j.bbamem.2004.05.011

Pitson, S.M., R.J. D'andrea, L. Vandeleur, P.A. Moretti, P. Xia, J.R. Gamble, M.A. Vadas, and B.W. Wattenberg. 2000a. Human sphingosine kinase: purification, molecular cloning and characterization of the native and recombinant enzymes. *Biochem. J.* 350:429–441. doi:10.1042/0264-6021:3500429

Pitson, S.M., P.A.B. Moretti, J.R. Zebol, P. Xia, J.R. Gamble, M.A. Vadas, R.J. D'Andrea, and B.W. Wattenberg. 2000b. Expression of a catalytically inactive sphingosine kinase mutant blocks agonist-induced sphingosine kinase activation. A dominant-negative sphingosine kinase. *J. Biol. Chem.* 275:33945–33950. doi:10.1074/jbc.M006176200

Pyne, N.J., J.S. Long, S.C. Lee, C. Loveridge, L. Gillies, and S. Pyne. 2009. New aspects of sphingosine 1-phosphate signaling in mammalian cells. *Adv. Enzyme Regul.* 49:214–221. doi:10.1016/j.advenzreg.2009.01.011

Raghu, P., K. Usher, S. Jonas, S. Chyb, A. Polyanovsky, and R.C. Hardie. 2000. Constitutive activity of the light-sensitive channels TRP and TRPL in the *Drosophila* diacylglycerol kinase mutant, rdgA. *Neuron.* 26:169–179. doi:10.1016/S0896-6273(00)81147-2

Sanchez, T., and T. Hla. 2004. Structural and functional characteristics of S1P receptors. *J. Cell. Biochem.* 92:913–922. doi:10.1002/jcb.20127

Satoh, A.K., J.E. O'Tousa, K. Ozaki, and D.F. Ready. 2005. Rab11 mediates post-Golgi trafficking of rhodopsin to the photosensitive apical membrane of *Drosophila* photoreceptors. *Development.* 132:1487–1497. doi:10.1242/dev.01704

Schulze, H., T. Kolter, and K. Sandhoff. 2009. Principles of lysosomal membrane degradation: Cellular topology and biochemistry of lysosomal lipid degradation. *Biochim. Biophys. Acta.* 1793:674–683. doi:10.1016/j.bbamcr.2008.09.020

Scott, R.C., G. Juhász, and T.P. Neufeld. 2007. Direct induction of autophagy by Atg1 inhibits cell growth and induces apoptotic cell death. *Curr. Biol.* 17:1–11. doi:10.1016/j.cub.2006.10.053

Sevrioukov, E.A., J.P. He, N. Moghrabi, A. Sunio, and H. Krämer. 1999. A role for the deep orange and carnation eye color genes in lysosomal delivery in *Drosophila*. *Mol. Cell.* 4:479–486. doi:10.1016/S1097-2765(00)80199-9

Sriram, V., K.S. Krishnan, and S. Mayor. 2003. *deep-orange* and *carnation* define distinct stages in late endosomal biogenesis in *Drosophila melanogaster*. *J. Cell Biol.* 161:593–607. doi:10.1083/jcb.200210166

Trajkovic, K., C. Hsu, S. Chiantia, L. Rajendran, D. Wenzel, F. Wieland, P. Schwille, B. Brügger, and M. Simons. 2008. Ceramide triggers budding of exosome vesicles into multivesicular endosomes. *Science.* 319:1244–1247. doi:10.1126/science.1153124

Walther, R.F., and F. Pichaud. 2007. Immunofluorescent staining and imaging of the pupal and adult *Drosophila* visual system. *Nat. Protoc.* 1:2635–2642. doi:10.1038/nprot.2006.379

Wang, T., and C. Montell. 2007. Phototransduction and retinal degeneration in *Drosophila*. *Pflugers Arch.* 454:821–847. doi:10.1007/s00424-007-0251-1

Wang, T., H. Xu, J. Oberwinkler, Y. Gu, R.C. Hardie, and C. Montell. 2005. Light activation, adaptation, and cell survival functions of the Na+/Ca2+ exchanger CalX. *Neuron.* 45:367–378. doi:10.1016/j.neuron.2004.12.046

Xu, H., S.J. Lee, E. Suzuki, K.D. Dugan, A. Stoddard, H.S. Li, L.A. Chodosh, and C. Montell. 2004. A lysosomal tetraspanin associated with retinal degeneration identified via a genome-wide screen. *EMBO J.* 23:811–822. doi:10.1038/sj.emboj.7600112